

# Two-dimensional ferromagnetic materials and related van der Waals heterostructures: a first-principle study

Baoxing Zhai<sup>1</sup>, Juan Du<sup>2</sup>, Xueping Li<sup>3</sup>, Congxin Xia<sup>1,†</sup>, and Zhongming Wei<sup>4,†</sup>

<sup>1</sup>Department of Physics, Henan Normal University, Xinxiang 453007, China

<sup>2</sup>State Key Laboratory for Artificial Microstructures and Mesoscopic Physics, School of Physics, Peking University, Beijing 100871, China

<sup>3</sup>College of Electronic and Electrical Engineering, Henan Normal University, Xinxiang 453007, China

<sup>4</sup>Institutes of Semiconductors, Chinese Academy of Sciences, Beijing 100083, China

**Abstract:** Since the successful fabrication of two-dimensional (2D) ferromagnetic (FM) monolayer  $\text{CrI}_3$  and  $\text{Cr}_2\text{Ge}_2\text{Te}_6$ , 2D FM materials are becoming an exciting research topic in condensed matter physics and materials fields, as they provide a good platform to explore the fundamental physical properties of magnetic materials under 2D limit. In this review, we summarize the theoretical research progress of intrinsic 2D FM materials and related van der Waals heterostructures (vdWHs) including their electronic structures, magnetism, Curie temperature, valley polarization, and band alignment. Moreover, we also summarize recent researches on the methods that used to regulate the above properties of 2D FM materials and vdWHs, such as defects, doping, strain, electric field and interlayer coupling. These studies show that 2D FM materials have broad application prospects in spintronics and valleytronics. However, there are still many problems waiting to be solved on the way to practical application.

**Key words:** 2D FM materials; heterostructure; Curie temperature

**Citation:** B X Zhai, J Du, X P Li, C X Xia, and Z M Wei, Two-dimensional ferromagnetic materials and related van der Waals heterostructures: a first-principle study[J]. *J. Semicond.*, 2019, 40(8), 081509. <http://doi.org/10.1088/1674-4926/40/8/081509>

## 1. Introduction

Because of the prediction of Landau, people are always uncertain of the existence of two-dimensional (2D) materials before graphene was exfoliated successfully<sup>[1]</sup>. Also for 2D ferromagnetic (FM) materials, the famous Mermin-Wagner theorem points out: Long-range magnetic order of isotropic spin-S Heisenberg model does not exist at nonzero temperature in dimensions  $d \leq 2$ <sup>[2]</sup>, which discourages many people who want to study 2D ferromagnets. However, people have not completely given up looking for 2D ferromagnets. After unremitting research, it has been found that magnetism can be induced in 2D systems by some external conditions, such as doping<sup>[3–5]</sup> and defects<sup>[6, 7]</sup>. Until 2017, 2D FM monolayer  $\text{CrI}_3$ <sup>[8]</sup> and  $\text{Cr}_2\text{Ge}_2\text{Te}_6$ <sup>[9]</sup> were successfully fabricated in experiments, which has attracted extensive attention. Massive researches on monolayer  $\text{CrI}_3$  and  $\text{Cr}_2\text{Ge}_2\text{Te}_6$  are beginning to emerge<sup>[10–17]</sup>. People have regained confidence and enthusiasm for the study of 2D ferromagnet. Recently, new 2D FM materials have been constantly predicted theoretically and synthesized experimentally, such as  $\text{Fe}_3\text{GeTe}_2$ <sup>[18]</sup>,  $\text{VSe}_2$ <sup>[19]</sup>,  $\text{MnSe}_2$ <sup>[20]</sup>,  $\text{Fe}_3\text{P}$ <sup>[21]</sup>,  $\text{VI}_3$ <sup>[22]</sup>, and so on. The appearance of 2D FM materials provides a good platform for people to study physical properties of magnetic materials under 2D limit.

The appearance of van der Waals heterostructure (vdWH) engineering is accompanied by the in-depth study of 2D materials<sup>[23]</sup>. Just like building blocks<sup>[24]</sup>, people can stack different ma-

terials to form heterostructures at will under the premise of lattice matching. The heterostructures usually show novel properties which are different from those of compositional materials and we can learn it from studying the charge transfer<sup>[17]</sup>, exciton state<sup>[25–27]</sup>, band alignment<sup>[17, 28, 29]</sup> and so on. With the emergence of 2D FM materials, we have more choices to construct heterostructures. We can't help thinking that what novel properties would exhibit when a traditional non-magnetic material, such as TMDC, graphene, came into contact with a magnetic material. In fact, this topic is not fresh, and the magnetic and non-magnetic interface engineering, such as  $\text{MoTe}_2/\text{EuO}$ <sup>[30]</sup>,  $\text{MoS}_2/\text{EuS}$ <sup>[31]</sup>,  $\text{WS}_2/\text{MnO}$ <sup>[32]</sup>, has been studied before. However, due to the uncertainty of 2D magnet before, the problem was most studied in the mixed dimensional heterostructures (2D/3D) composed of 2D nonmagnetic materials and magnetic bulk materials.

In this review, we summarize recent researches on 2D FM materials and 2D FM vdWHs, including the intrinsic physical properties of 2D FM monolayers and 2D FM vdWHs, as well as the regulation of physical properties by some external conditions such as defect, doping, strain, and electric field. We also discuss the developing trend of 2D FM monolayers and vdWHs. We believe that it can help readers to further understand 2D FM materials.

## 2. Research about 2D FM materials

### 2.1. Intrinsic physical properties of 2D FM materials

We first show the crystal model of  $\text{CrI}_3$  and  $\text{Cr}_2\text{Ge}_2\text{Te}_6$  in Fig. 1(a). It can be seen that the atomic structure of  $\text{CrI}_3$  is simpler, which means that it has higher symmetry. And Figs. 1(b) and 1(c) display the band structures of monolayer  $\text{CrI}_3$  and  $\text{Cr}_2\text{Ge}_2\text{Te}_6$ , respectively, from which we can see that these two

Correspondence to: C X Xia, [xiacongxin@htu.edu.cn](mailto:xiacongxin@htu.edu.cn); Z M Wei, [zmwei@semi.ac.cn](mailto:zmwei@semi.ac.cn)

Received 2 JUNE 2019; Revised 8 JULY 2019.

©2019 Chinese Institute of Electronics

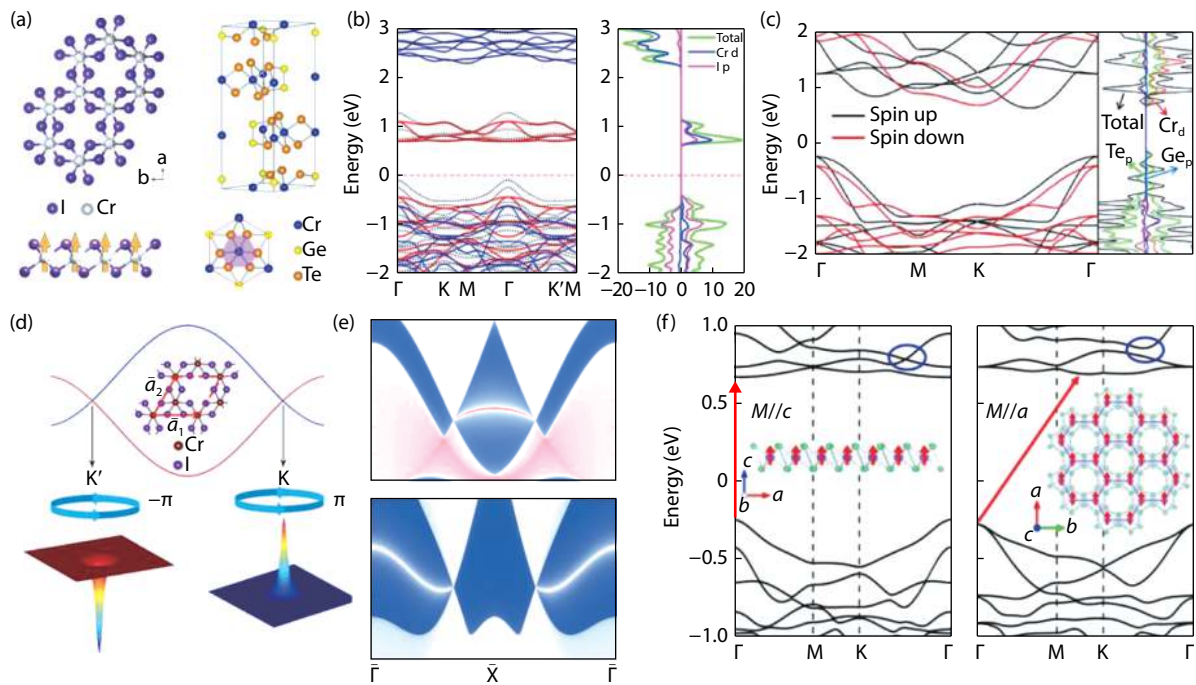


Fig. 1. (Color online) (a) The structure diagram of monolayer  $\text{CrI}_3$  (left) and monolayer  $\text{Cr}_2\text{Ge}_2\text{Te}_6$  (right). Reprinted with permission from Refs. [8, 9]. Copyright 2017, Springer Nature. The band structures and density of state (DOS) of (b)  $\text{CrI}_3$  and (c)  $\text{Cr}_2\text{Ge}_2\text{Te}_6$ . Reprinted with permission from Ref. [17]. Copyright 2019, AIP Publishing. (d) The distributions of phonon Berry curvature near two inequivalent valleys K and K', respectively, indicating that a phonon Dirac point is a singularity in momentum space. (e) The LDOS projected on edges of semi-infinite nanoribbons of (top)  $\text{CrI}_3$  and (down) YGaI along the zigzag direction. The nontrivial edge states terminated at the projection of phonon Dirac cones are clearly visible. Reprinted with permission from Ref. [34]. Copyright 2018, American Chemical Society (f) The band structure with magnetic moment along the out-of-plane  $c$  axis (left) and in-plane  $a$  axis (right). The red arrows depict the band gap that is direct with  $M//c$  and indirect with  $M//a$ . The insets show the side view and top view of the crystal structure with spin orientation along the  $c$  axis and  $a$  axis, respectively. Reprinted with permission from Ref. [33]. Copyright 2018, American Chemical Society.

monolayers are both ferromagnetic semiconductors. Also, their Curie temperature ( $T_c$ ) and magnetic anisotropy have been systematically studied [8, 9]. In addition, Zhong *et al.* find that the monolayer  $\text{CrI}_3$  possesses a giant magneto band-structure effect, i.e. the change of spin orientation can significantly modify the band structure of this material. Here, rotating the magnetic moment of  $\text{CrI}_3$  from out-of-plane to in-plane will cause a direct-to-indirect bandgap transition (Fig. 1(f)), which can result in a magnetic field controlled photoluminescence. They also find a significant change of Fermi surface with different magnetization directions, giving rise to giant anisotropic magnetoresistance. Moreover, the spin reorientation is found to modify the topological states [33]. Their work opens a new paradigm for spintronics applications. Xu *et al.* have studied phonon edge states and phonon Berry Phase with the monolayer  $\text{CrI}_3$  as a platform through first-principles calculations. They find that the phonon Berry phase is quantized to  $\pm \pi$  at two inequivalent valleys and the phonon edge states terminated at the projection of phonon Dirac cones (Figs. 1(d) and 1(e)). This work extends the knowledge of valley physics, providing wide applications of topological phonons [34].

## 2.2. Regulation of physical properties of 2D FM materials

In addition to study the intrinsic physical properties of two-dimensional ferromagnet, it is also very important to study the effects of external conditions such as the defect [35],

charge doping [14, 36], electric field [13, 17, 37] and strain [17, 38] on its physical properties, such as electronic structure, magnetic anisotropy,  $T_c$  and so on. Wang *et al.* find that the I vacancies on the surface of monolayer  $\text{CrI}_3$  can not only enhance the intrinsic ferromagnetism of monolayer  $\text{CrI}_3$  but also induce switchable out-of-plane electric polarization (Fig. 2(a)), and the I vacancies do not break the semiconducting nature of  $\text{CrI}_3$ . In addition, they also find that the polarization direction can be reversed by switching the position of I vacancies and this method is also applicable to many other metal trihalides [35]. This work provides a new way for people to realize and regulate the electric polarization in low-dimensional systems, which is meaningful for engineering the multifunctional nanodevices. According to the study of Wu *et al.*, now we have already known that electron or hole doping can transform  $\text{CrI}_3$  from semiconductor to metal, and improve the stability of its FM ground state [36], see Figs. 2(b) and 2(c). In addition, the electronic structure and the magnetism regulation of the 2D ferromagnet can also be realized by the strain engineering and the external electric field [17], see Figs. 2(d) and 2(e). For example, Gong *et al.* found that by applying a vertical electric field, the bilayer  $\text{VS}_2$  can convert from A type antiferromagnet to half metal. Fig. 2(f) shows the side view of bilayer  $\text{VS}_2$ . The regulation of the electric field on the energy levels shows the opposite trends in different spin channels, leading to the gradual decrease of the gap of spin- $\alpha$  states and the opening of the gap of the spin- $\beta$  states [37]. When the electric field reaches a cer-

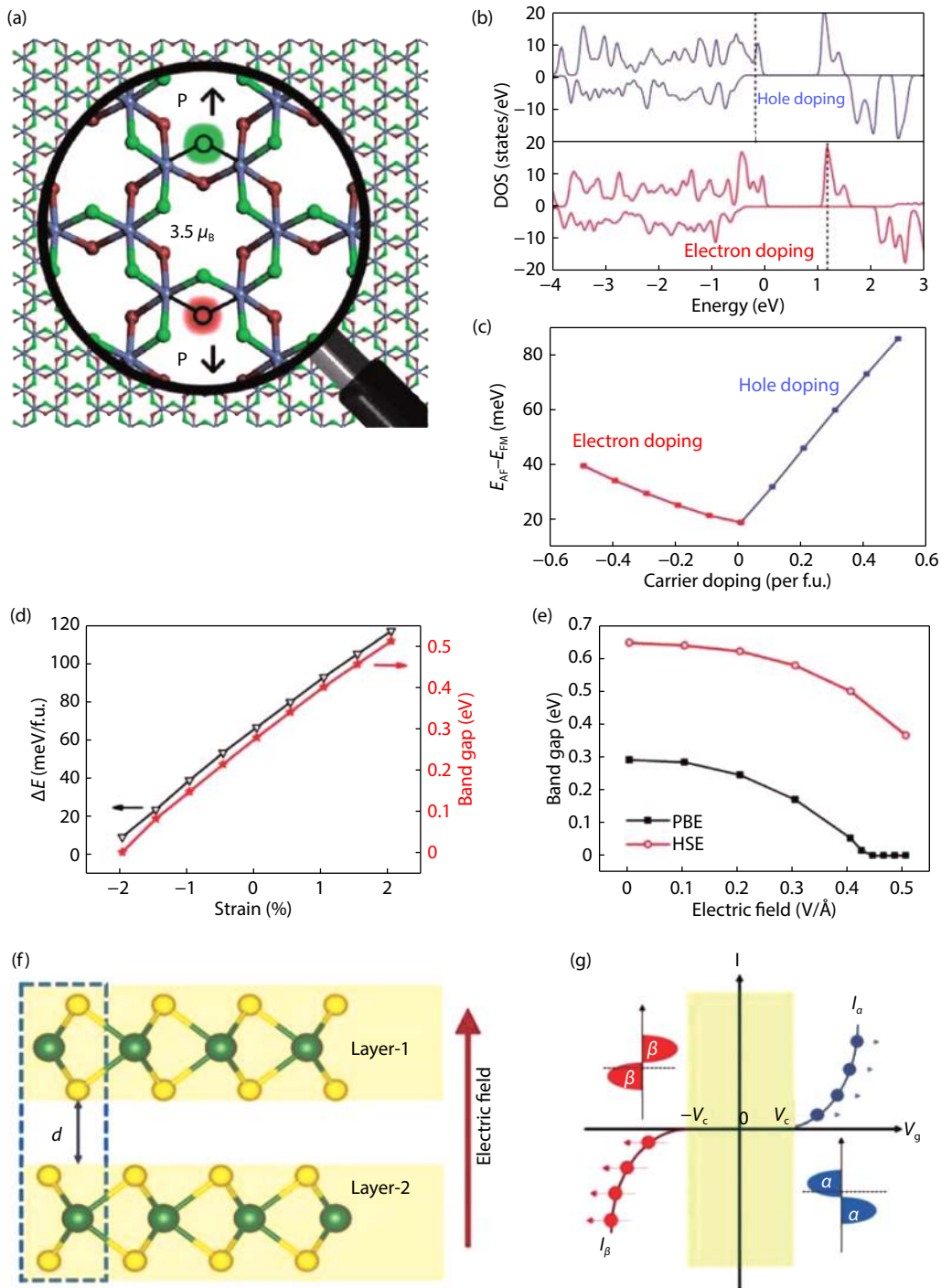


Fig. 2. (Color online) (a) The I-vacancies models of monolayer CrI<sub>3</sub>. Reprinted with permission from Ref. [35]. Copyright 2018, American Chemical Society. (b) The DOS of CrI<sub>3</sub> monolayer doped with 0.5 hole or 0.5 electron, and (c) Relationship between ferromagnetic stability and carrier doping concentration. The dashed vertical lines in (b) refer to the shifting Fermi level<sup>[36]</sup>. (d) The strain engineering of monolayer Cr<sub>2</sub>Ge<sub>2</sub>Te<sub>6</sub> shows that the bandgaps vary with the increase of biaxial strain for the FM state (the red line), and the black line represents the variety of total energy difference between the AFM and FM configurations with the strain in the monolayer Cr<sub>2</sub>Ge<sub>2</sub>Te<sub>6</sub>. (e) The dependence of PBE and HSE06 bandgaps under a perpendicular electric field with different field strengths. Reprinted with permission from Ref. [17]. Copyright 2019, AIP Publishing. (f) The side view of the bilayer 2H-VSe<sub>2</sub>, with the electric field applied perpendicularly from layer 2 to layer 1. (g) The schematic spin-polarized current versus the gate voltage, with  $V_c$  indicating the critical voltage. The switching of the spin- $\alpha$  current  $I_\alpha$  and spin- $\beta$  current  $I_\beta$  can be manipulated by the gate voltage. Reprinted with permission from Ref. [37]. Copyright 2017, National Academy of Sciences.

tain value, the band gap of one spin state is zero, while the other spin state is still an insulated state. Thus, the 100% spin polarization current will be generated in bilayer VS<sub>2</sub>, see Fig. 2(g). Their research is very meaningful for designing the spin field ef-

fect transistor. What's more, Wu *et al.* also point out that the energy difference between FM state and AFM state directly corresponds to the  $T_c$ <sup>[36]</sup>. From this we can conclude that the above methods can certainly change the  $T_c$  of the material. And in ex-

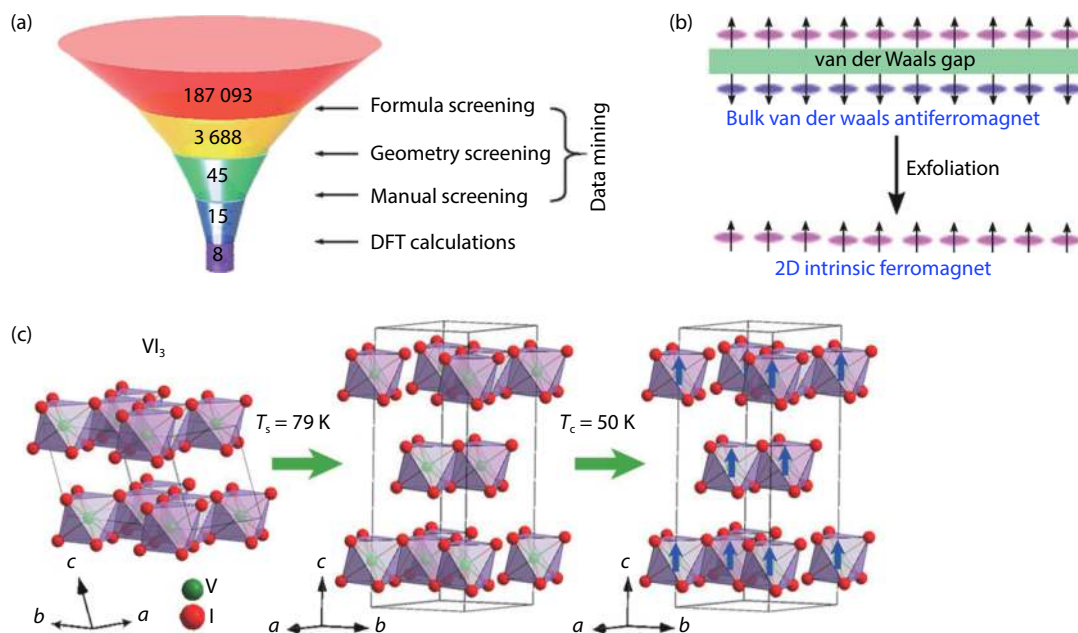


Fig. 3. (Color online) (a) A schematic diagram to illustrate the search procedure for 2D FM materials. Reprinted with permission from Ref. [41]. Copyright 2018, American Physical Society. (b) A schematic diagram to obtain the 2D intrinsic ferromagnet from the van der Waals antiferromagnetic bulk. Reprinted with permission from Ref. [42]. Copyright 2018, American Chemical Society. (c) the monolayer  $\text{VI}_3$  be exfoliated from the bulk  $\text{VI}_3$ . Reprinted with permission from Ref. [22]. Copyright 2019, American Chemical Society.

periment, Zhang *et al.* have proved that the  $T_c$  of  $\text{Fe}_3\text{GeTe}_2$  can be increased to room temperature by electric field<sup>[18]</sup>. In addition, the regulation of 2D ferromagnetism by external electric field<sup>[13]</sup> and electrostatic doping<sup>[14]</sup> has been realized experimentally.

Through these studies, we can see that FM materials under 2D limit possess unusual properties in many aspects. I believe this will attract more and more attention, and there will be more groundbreaking and meaningful results in the future.

### 2.3. More 2D FM materials with higher $T_c$

Compared with the past, people simply obtained a kind of new material or a class of new materials by atomic substitution, but now people have begun to search for new 2D materials quickly and systematically using high-throughput calculation methods<sup>[39–41]</sup> such as structure search, machine learning and the like. Moreover, we can further screen 2D FM materials with excellent performance from the database through formula screening, geometry screening, manual screening and DFT calculations (Fig. 3(a)).

At present, people have gradually established a 2D material database<sup>[39]</sup>, and are still trying to discover new 2D ferromagnets from theory and experiment. As shown in Fig. 3(b), Sun *et al.* theoretically find a class of new 2D ferromagnets,  $\text{CrOCl}$  and  $\text{CrOBr}$  monolayers, which can be obtained by exfoliating from the layered AFM bulk materials<sup>[42]</sup>. Also, Lei *et al.* successfully synthesize vdW magnetic compound  $\text{VI}_3$  in experiment, and theoretically predict that the monolayer  $\text{VI}_3$  possesses the ferromagnetic-insulator property and are feasible to be exfoliated from the bulk<sup>[22]</sup> (Fig. 3(c)). It can be seen that the combination of theoretical prediction and experimental verification will greatly accelerate the research process of 2D FM materials, and there will be more and more 2D FM materials be made in the future.

Although there are many 2D FM materials predicted by theory, very few have been successfully prepared in experiments,

and most of the  $T_c$  are much lower than room temperature, such as monolayer  $\text{CrI}_3$  ( $T_c = 45 \text{ K}$ )<sup>[8]</sup>,  $\text{Cr}_2\text{Ge}_2\text{Te}_6$  ( $T_c = 28 \text{ K}$ )<sup>[9]</sup>,  $\text{Fe}_3\text{GeTe}_2$  ( $T_c \approx 19 \text{ K}$ )<sup>[18]</sup>, which will limit the application of these materials in pragmatic spintronic devices. Therefore, it is urgent to find 2D FM materials with the higher  $T_c$  and the method of raising the  $T_c$ . The Journal of Science has published 125 of the most important issues, one of which is whether it is possible to produce a room-temperature FM semiconductor<sup>[43]</sup>. Recently, some research progress has been made in these areas.

In theory, Zhao *et al.* systematically screen out five high temperature 2D FM materials ( $\text{LaCl}$ ,  $\text{YCl}$ ,  $\text{ScCl}$ ,  $\text{LaBr}_2$ , and  $\text{CrSBr}$  with  $T_c > 200 \text{ K}$ ) using the first-principle calculation methods<sup>[44]</sup>, see Fig. 4(a). Kan *et al.* propose a method to raise the  $T_c$ . As shown in Fig. 4(b), they found that in double-orbital model, the ferromagnetism of the material is closely related to the virtual exchange gap. Thus, we can reduce the exchange gap by equivalent alloying the material, which can greatly enhance the FM coupling. They also validated the proposed theory with  $\text{CrI}_3$ ,  $\text{CrGeTe}_3$  and so on, and the results show that their  $T_c$  is increased by 3–5 times by alloying<sup>[45]</sup>. In addition, Yang *et al.* also raise a method to achieve high  $T_c$ . They design a special organometallic frameworks connected by antiaromatic rings, which can enhance the  $T_c$  of 2D FM semiconductors much higher than room temperature<sup>[46]</sup>, see Figs. 4(c)–4(e).

In experiments, it has been mentioned that different research groups have tried to increase  $T_c$  of materials through some external conditions. At the same time, people are trying to explore new 2D intrinsic ferromagnetic materials with room temperature. For example,  $\text{VSe}_2$  and  $\text{MnSe}_2$  monolayers have been successfully obtained in experiments, and the results show that they have high  $T_c$  with 330 K for  $\text{VSe}_2$  and 300 K for  $\text{MnSe}_2$ <sup>[19, 20]</sup>.

### 3. 2D FM vdWHs

Not only 2D ferromagnets themselves have many novel

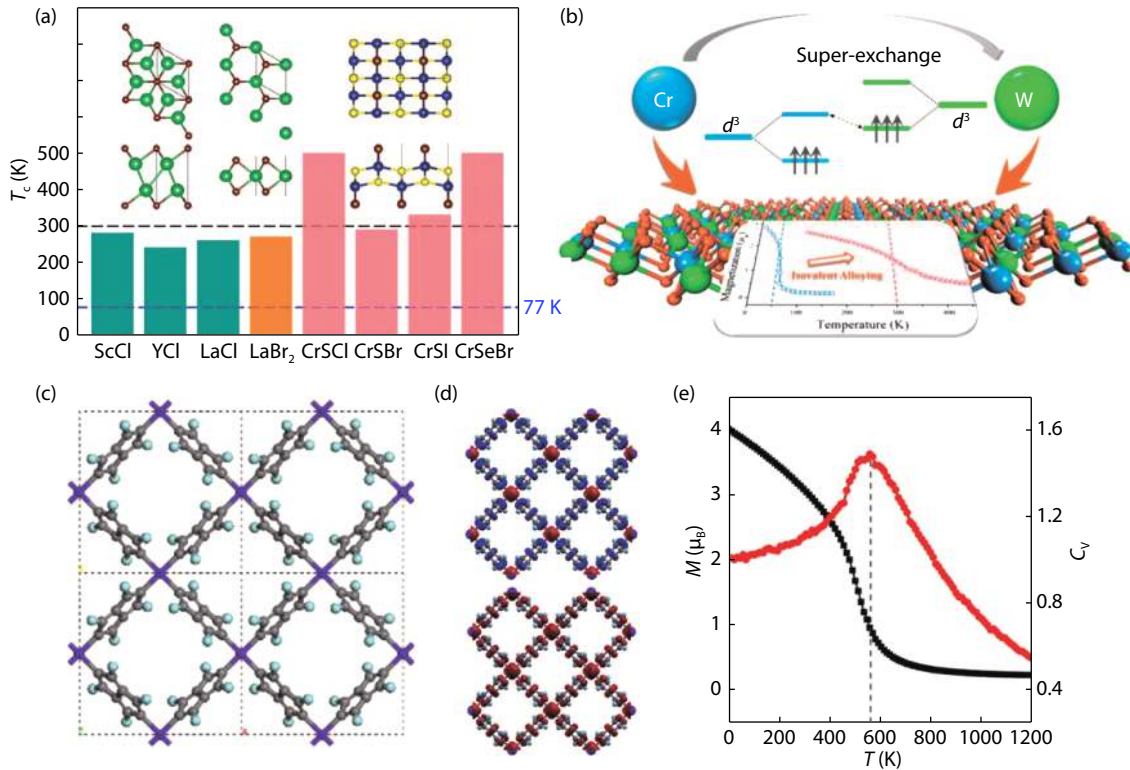


Fig. 4. (Color online) (a) The diagram of  $T_c$  and structural models of several high temperature FM materials. Reprinted with permission from Ref. [44]. Copyright 2018, American Chemical Society. (b) the mechanism of superexchange in two semiconducting alloy compounds CrW<sub>6</sub> and CrWGe<sub>2</sub>Te<sub>6</sub> monolayers. The insert is the enhanced  $T_c$  of CrW<sub>6</sub> and CrWGe<sub>2</sub>Te<sub>6</sub> compared to 2D CrI<sub>3</sub> and CrGeTe<sub>3</sub>. Reprinted with permission from Ref. [45]. Copyright 2018, American Chemical Society. (c) The structural model of metal organic framework. (d) Spin density of ferrimagnetic (top) and FM (bottom) coupling for 2D Cr-pentalene with an isovalue of 0.05 e/Å<sup>3</sup>. Red and blue indicate spin up and spin down, respectively. (e) Variation of magnetic moment ( $M$ ) per unit cell (black) and specific heat ( $C_V$ ) (red) with respect to temperature from classic Heisenberg model Monte Carlo simulation. Reprinted with permission from Ref. [46]. Copyright 2018, American Chemical Society.

physical properties, but also many novel physical phenomena will appear when they are stacked with other nonmagnetic 2D materials, such as proximity induced spin polarization<sup>[47, 48]</sup>, valley polarization<sup>[49, 50]</sup>, and topological properties<sup>[51, 52]</sup>. Now, more and more people have started to study 2D FM vdWHs. Very recently, Zhang *et al.* have summarized several factors related to the interface engineering of magnetic heterostructures in a review<sup>[53]</sup>. So we will not describe it here. In this section, we focus on the theoretical works on 2D FM vdWHs, hoping to help readers further understand this direction.

### 3.1. Spin-polarized band structures

When the ferromagnetic materials and non-magnetic materials are stacked forming the vdWHs, due to the spin-polarized electronic structure of magnetic materials, the heterostructures will also possess different electronic states in different spin channels. As shown in Fig. 5(a), the Mg(OH)<sub>2</sub>/VS<sub>2</sub> vdWH possess the spin-polarized band structure with the conduction-band maximum (CBM) are located at K and M point in the spin-up channel and spin-down channel, respectively. Obviously, the band gaps of different spin channels are different with 0.14 eV for spin up and 0.57 eV for spin down. Moreover, it can also be seen from the band alignment that there are different band offsets in different spin channels, see Fig. 5(b), which means that there are different separation possibilities for electrons and holes in spin-up and spin-down channels. In addition, Xiong *et al.* also found that the external electric field can

induce the different band-alignment transition in different spin channels<sup>[47]</sup> (Fig. 5(c)). The characteristic of multiple-band alignments induced by electric field potentially prompts a new type of multifunctional spintronic device.

### 3.2. Valley polarization and quantum anomalous Hall effect

More and more attention has been paid for the valley-physics properties of graphene and monolayer transition metal dichalcogenides (TMDC) MX<sub>2</sub> ( $M = \text{Mo, W}$ ;  $X = \text{S, Se, Te}$ ). Compared with graphene, the monolayer MX<sub>2</sub> have stronger spin orbit coupling (SOC) effect, which leads to obvious energy level splitting at K and K' valleys, and these two valleys are energetically degenerate because of the time-reversal symmetry. Also, the broken inversion symmetry features two inequivalent valleys with different angular momenta, as shown in Fig. 6(a). Based on the above factors, we can implement the valley hall effect in monolayer MX<sub>2</sub> where carriers in different valleys flow to opposite transverse edges when applying an in-plane electric field<sup>[54]</sup>. In addition, when we somehow produce a non-zero net magnetic moment in this material, the valley degeneracy can be lifted (Fig. 6(b)), which we call the valley polarization. At present, several methods are often used to realize valley polarization, such as optical pumping<sup>[55]</sup>, external magnetic field<sup>[56]</sup>, doping magnetic atoms<sup>[57]</sup>, stacking on magnetic materials<sup>[30–32]</sup>. Among them, constructing FM vdWHs is a very promising method because it is more stable and easier to

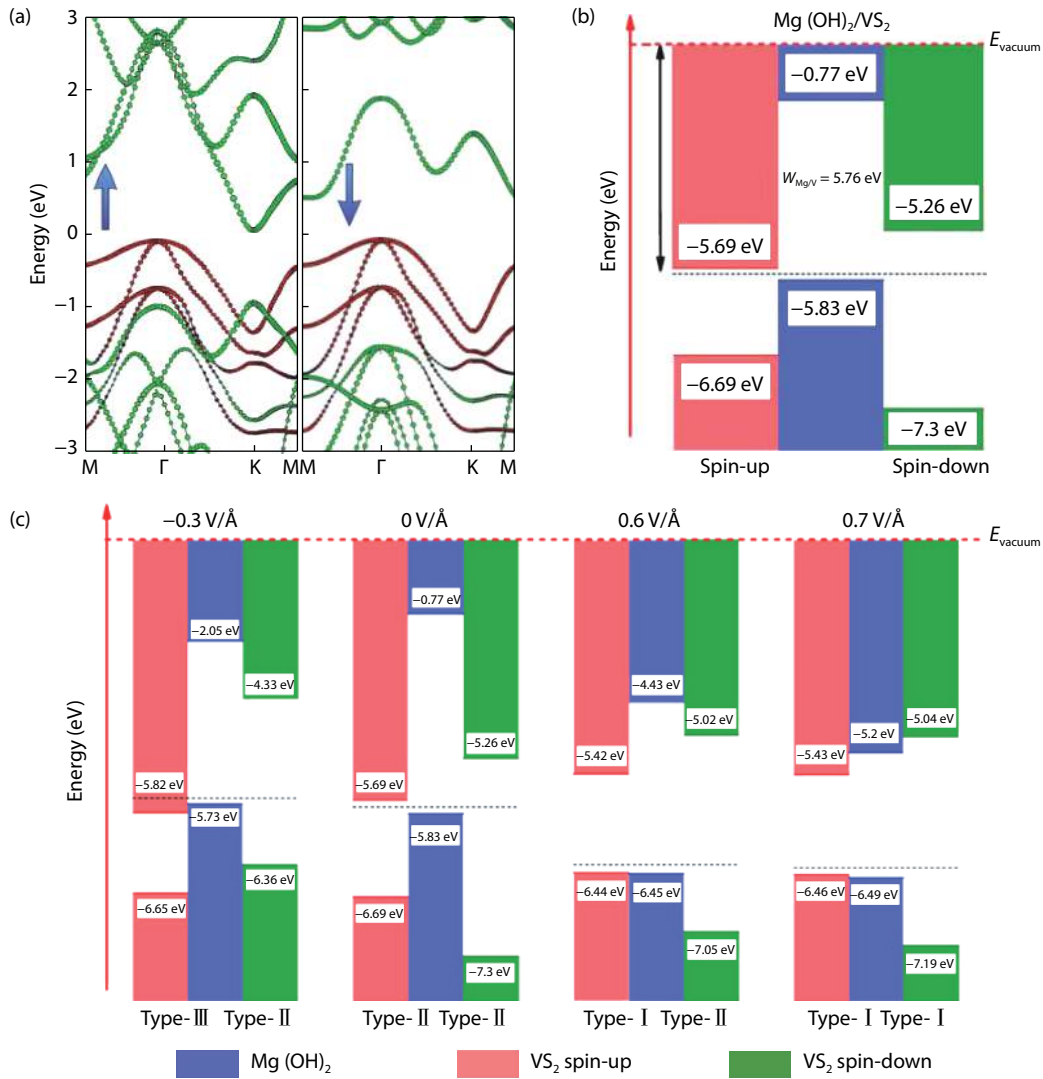


Fig. 5. (Color online) (a) The spin-polarized band structure of Mg(OH)<sub>2</sub>/VS<sub>2</sub> heterostructure. (b) The band alignment and work function of the heterostructure, referring to the vacuum level ( $E_{\text{vacuum}}$ ). (c) Band alignments of Mg(OH)<sub>2</sub>/VS<sub>2</sub> heterostructure at various electric field values:  $-0.3$ ,  $0$ ,  $0.6$ , and  $0.7$  V/Å, respectively, referring to the  $E_{\text{vacuum}}$ . Reprinted with permission from Ref. [47]. Copyright 2017, American Physical Society.

regulate.

With the emergence of 2D FM materials, people began to study the valley polarization in 2D/2D systems. Recently, Liu *et al.* have studied the effect of stacking mode on valley polarization in WSe<sub>2</sub>/CrI<sub>3</sub> vdWH<sup>[49]</sup>, and Farooq *et al.* found that the valley polarization also exists in graphene/CrI<sub>3</sub> and bilayer graphene/CrI<sub>3</sub> vdWHs, and the valley-polarization characteristics can be regulated by electric field<sup>[50]</sup>, see Figs. 6(c) and 6(d). In addition, it is also in graphene/CrI<sub>3</sub> vdWH, a Chern insulating state can be acquired if the interlayer distance is compressed to a distance between about 3.3 and 2.4 Å, and the quantum anomalous Hall effect (QAHE) is promising to be observed<sup>[51]</sup> (Figs. 6(e) and 6(f)). Very recently, the high-temperature QAHE also has been predicted existing in 2D germanene/Cr<sub>2</sub>Ge<sub>2</sub>Te<sub>6</sub> and germanene/CrI<sub>3</sub> vdWHs<sup>[52]</sup>. These results show that there are still many physics waiting for us to discover in 2D FM vdWH systems. In addition, they also point out the direction for the experimental study of 2D FM vdWHs.

We also note that a new type of multiferroic vdWHs has recently been proposed<sup>[58, 59]</sup>. Multiferroic means that one material has two or more properties of ferroelectricity, ferromagnet-

ism and ferroelasticity at the same time. However, very few intrinsic multiferroic materials have been found, which limits the research of this direction and the development of multifunctional nano-electronic devices. Now, we can simply stack a 2D FM material with a 2D ferroelectric material to form a multiferroic heterostructure, which may provide a new way for people to achieve multiferroic in experiments.

#### 4. Conclusion

In conclusion, we summarize the recent theoretical advances on intrinsic 2D FM materials and vdWHs, including the intrinsic electronic structure, magnetism,  $T_C$ , valley polarization, band alignment and so on. These studies show that 2D FM materials and vdWHs possess many novel physical properties, and they are promising materials to be applied in spintronic and valleytronic nanodevices. Moreover, many methods, such as vacancy, doping, strain and external electrical field, can be used to regulate the electronic structure, magnetism,  $T_C$ , valley polarization, and band alignment of 2D FM materials and vdWHs, indicating the properties of 2D FM materials and vdWHs are highly tunable. However, although many 2D FM materials

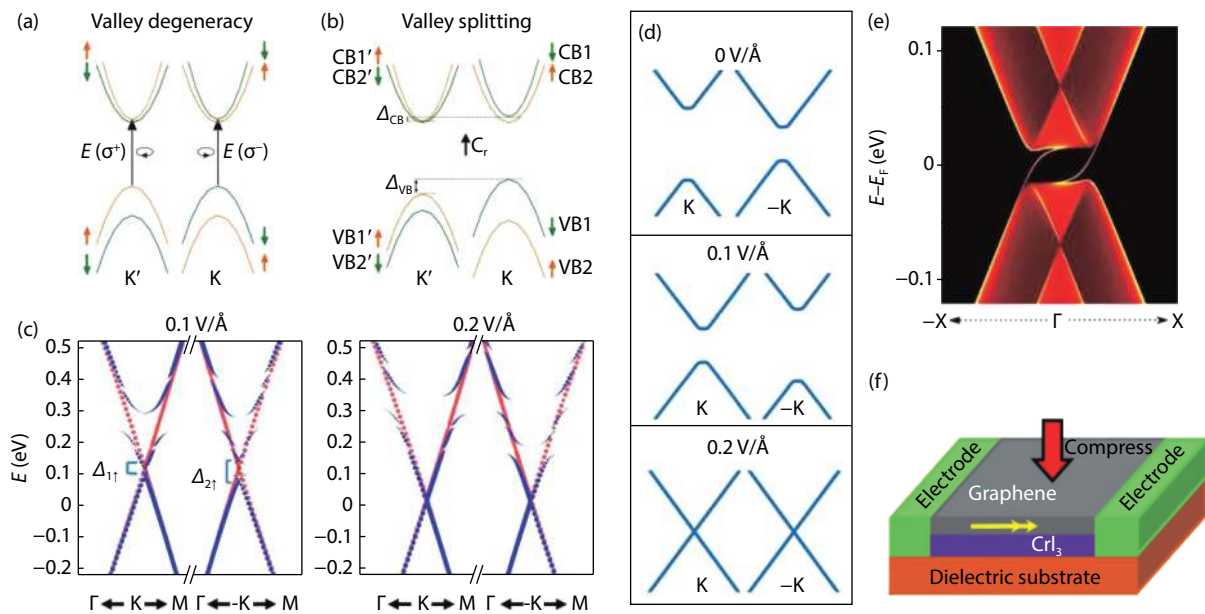


Fig. 6. (Color online) (a) The energy diagram of the monolayer  $WSe_2$  at the  $K, K'$  valleys.  $E(\sigma^+)$  and  $E(\sigma^-)$  represent the interband optical transition energies of right-hand ( $\sigma^+$ ) and left-hand ( $\sigma^-$ ) circularly polarized photons, respectively. The spin-up and spin-down valley-spin states are denoted with orange up- and green down-arrows, respectively. (b) Energy diagram depicting the  $K$  and  $K'$  valley degeneracy lifting. The VB and CB stand for the valence and conduction band valley splittings, respectively. The black-up arrow denotes the Cr spin is aligned vertically upward, i.e., the magnetization axis of the  $CrI_3$ . Reprinted with permission from Ref. [49]. Copyright 2019, American Physical Society. (c) projection bands of graphene around  $\pm K$  with SOC under the electric field. (d) schematics illustration of change of valley splitting at  $\pm K$  under the electric field. Reprinted with permission from Ref. [51]. Copyright 2019, Springer Nature. (e) The calculated edge density of states of the semi-infinite armchair-edged graphene system. (f) A schematic diagram depicting the observation of the QAH effect in graphene/ $CrI_3$  heterobilayer. The vertical red arrow denotes the external compression. The small horizontal yellow arrows indicate the two dissipationless edge current channels owned in the heterostructure. Reprinted with permission from Ref. [51]. Copyright 2018, American Physical Society.

have been predicted in theory, very few of them have been successfully prepared in experiments. In addition, most  $T_c$  of 2D FM materials are much lower than room temperature, which limit the applications of these materials in practice. Therefore, it is necessary to find the 2D FM materials with the higher  $T_c$  or find the method of raising the  $T_c$ . In short, although we have made many breakthroughs in this field recently, there are still many problems waiting for us to find and solve.

## References

- [1] Novoselov K S, Geim A K, Morozov S V, et al. Electric field effect in atomically thin carbon films. *Science*, 2004, 306, 666
- [2] Mermin N D, Wagner H. Absence of ferromagnetism or antiferromagnetism in one- or two-dimensional isotropic Heisenberg models. *Phys Rev Lett*, 1966, 17, 1133
- [3] Zheng H, Yang B, Wang D, et al. Tuning magnetism of monolayer  $MoS_2$  by doping vacancy and applying strain. *Appl Phys Lett*, 2014, 104, 132403
- [4] Hashmi A, Hong J. Transition metal doped phosphorene: first-principles study. *J Phys Chem C*, 2015, 119, 9198
- [5] Du J, Xia C, An Y, et al. Tunable electronic structures and magnetism in arsenene nanosheets via transition metal doping. *J Mater Sci*, 2016, 51, 9504
- [6] Yazyev O V, Helm L. Defect-induced magnetism in graphene. *Phys Rev B*, 2007, 75, 125408
- [7] Nair R R, Sepioni M, Tsai I L, et al. Spin-half paramagnetism in graphene induced by point defects. *Nat Phys*, 2012, 8, 199
- [8] Huang B, Clark G, Navarro-Moratalla E, et al. Layer-dependent ferromagnetism in a van der Waals crystal down to the monolayer limit. *Nature*, 2017, 546, 270
- [9] Gong C, Li L, Li Z, et al. Discovery of intrinsic ferromagnetism in two-dimensional van der Waals crystals. *Nature*, 2017, 546, 265
- [10] Song T, Cai X, Tu M W Y, et al. Giant tunneling magnetoresistance in spin-filter van der Waals heterostructures. *Science*, 2018, 360, 1214
- [11] Seyler K L, Zhong D, Klein D R, et al. Ligand-field helical luminescence in a 2D ferromagnetic insulator. *Nat Phys*, 2018, 14, 277
- [12] Cardoso C, Soriano D, Garcia-Martinez N A, et al. Van der Waals spin valves. *Phys Rev Lett*, 2018, 121, 067701
- [13] Jiang S, Shan J, Mak K F. Electric-field switching of two-dimensional van der Waals magnets. *Nat Mater*, 2018, 17, 406
- [14] Jiang S, Li L, Wang Z, et al. Controlling magnetism in 2D  $CrI_3$  by electrostatic doping. *Nat Nanotechnol*, 2018, 13, 549
- [15] Lin G T, Luo X, Chen F C, et al. Critical behavior of two-dimensional intrinsically ferromagnetic semiconductor  $CrI_3$ . *Appl Phys Lett*, 2018, 112, 072405
- [16] Xu C, Feng J, Xiang H, et al. Interplay between Kitaev interaction and single ion anisotropy in ferromagnetic  $CrI_3$  and  $CrGeTe_3$  monolayers. *npj Comput Mater*, 2018, 4, 57
- [17] Wang K, Hu T, Jia F, et al. Magnetic and electronic properties of  $Cr_2Ge_2Te_6$  monolayer by strain and electric-field engineering. *Appl Phys Lett*, 2019, 114, 092405
- [18] Deng Y, Yu Y, Song Y, et al. Gate-tunable room-temperature ferromagnetism in two-dimensional  $Fe_3GeTe_2$ . *Nature*, 2018, 563, 94
- [19] Bonilla M, Kolekar S, Ma Y, et al. Strong room-temperature ferromagnetism in  $VSe_2$  monolayers on van der Waals substrates. *Nat Nanotechnol*, 2018, 13, 289
- [20] O'Hara D J, Zhu T, Trout A H, et al. Room temperature intrinsic ferromagnetism in epitaxial manganese selenide films in the monolayer limit. *Nano Lett*, 2018, 18, 3125

- [21] Zheng S, Huang C, Yu T, et al. High-temperature ferromagnetism in an Fe<sub>3</sub>P monolayer with a large magnetic anisotropy. *J Phys Chem Lett*, 2019, 10, 2733
- [22] Tian S, Zhang J-F, Li C, et al. Ferromagnetic van der Waals crystal V<sub>13</sub>. *J Am Chem Soc*, 2019, 141, 5326
- [23] Geim A K, Grigorieva I V. Van der Waals heterostructures. *Nature*, 2013, 499, 419
- [24] Yao S, Wang E, Zhou S. Van der Waals heterostructures, a new world in the field of two-dimensional materials. *Physics*, 2017, 5, 322
- [25] Unuchek D, Ciarrocchi A, Avsar A, et al. Room-temperature electrical control of exciton flux in a van der Waals heterostructure. *Nature*, 2018, 560, 340
- [26] Seyler K L, Rivera P, Yu H, et al. Signatures of moiré-trapped valley excitons in MoSe<sub>2</sub>/WSe<sub>2</sub> heterobilayers. *Nature*, 2019, 567, 66
- [27] Jin C, Regan E C, Yan A, et al. Observation of moiré excitons in WSe<sub>2</sub>/WS<sub>2</sub> heterostructure superlattices. *Nature*, 2019, 567, 76
- [28] Xia C, Xiong W, Du J, et al. Type-I transition metal dichalcogenides lateral homojunctions: layer thickness and external electric field effects. *Small*, 2018, 14, 1800365
- [29] Xia C, Du J, Li M, et al. Effects of electric field on the electronic structures of broken-gap phosphorene/SnX<sub>2</sub> (X = S, Se) van der Waals heterojunctions. *Phys Rev Appl*, 2018, 10, 054064
- [30] Qi J, Li X, Niu Q, et al. Giant and tunable valley degeneracy splitting in MoTe<sub>2</sub>. *Phys Rev B*, 2015, 92, 121403
- [31] Liang X, Deng L, Huang F, et al. The magnetic proximity effect and electrical field tunable valley degeneracy in MoS<sub>2</sub>/EuS van der Waals heterojunctions. *Nanoscale*, 2017, 9, 9502
- [32] Xu L, Yang M, Shen L, et al. Large valley splitting in monolayer WS<sub>2</sub> by proximity coupling to an insulating antiferromagnetic substrate. *Phys Rev B*, 2018, 97, 041405
- [33] Jiang P, Li L, Liao Z, et al. Spin direction-controlled electronic band structure in two-dimensional ferromagnetic CrI<sub>3</sub>. *Nano Lett*, 2018, 18, 3844
- [34] Jin Y, Wang R, Xu H. Recipe for Dirac phonon states with a quantized valley berry phase in two-dimensional hexagonal lattices. *Nano Lett*, 2018, 18, 7755
- [35] Zhao Y, Lin L, Zhou Q, et al. Surface vacancy-induced switchable electric polarization and enhanced ferromagnetism in monolayer metal trihalides. *Nano Lett*, 2018, 18, 2943
- [36] Wang H, Fan F, Zhu S, et al. Doping enhanced ferromagnetism and induced half-metallicity in CrI<sub>3</sub> monolayer. *EPL Europhys Lett*, 2016, 114, 47001
- [37] Gong S J, Gong C, Sun Y Y, et al. Electrically induced 2D half-metallic antiferromagnets and spin field effect transistors. *Proc Natl Acad Sci*, 2018, 115, 8511
- [38] Webster L, Yan J A. Strain-tunable magnetic anisotropy in monolayer CrCl<sub>3</sub>, CrBr<sub>3</sub>, and CrI<sub>3</sub>. *Phys Rev B*, 2018, 98, 144411
- [39] Hastrup S, Strange M, Pandey M, et al. The computational 2D materials database: high-throughput modeling and discovery of atomically thin crystals. *2D Mater*, 2018, 5, 042002
- [40] Mounet N, Gibertini M, Schwaller P, et al. Two-dimensional materials from high-throughput computational exfoliation of experimentally known compounds. *Nat Nanotechnol*, 2018, 13, 246
- [41] Zhu Y, Kong X, Rhone T D, et al. Systematic search for two-dimensional ferromagnetic materials. *Phys Rev Mater*, 2018, 2, 081001
- [42] Miao N, Xu B, Zhu L, et al. 2D intrinsic ferromagnets from van der Waals antiferromagnets. *J Am Chem Soc*, 2018, 140, 2417
- [43] So much more to know. *Science*, 2005, 309, 78b
- [44] Jiang Z, Wang P, Xing J, et al. Screening and design of novel 2D ferromagnetic materials with high Curie temperature above room temperature. *ACS Appl Mater Interfaces*, 2018, 10, 39032
- [45] Huang C, Feng J, Wu F, et al. Toward intrinsic room-temperature ferromagnetism in two-dimensional semiconductors. *J Am Chem Soc*, 2018, 140, 11519
- [46] Li X, Yang J. Realizing two-dimensional magnetic semiconductors with enhanced Curie temperature by antiaromatic ring based organometallic frameworks. *J Am Chem Soc*, 2019, 141, 109
- [47] Xiong W, Xia C, Du J, et al. Electrostatic gating dependent multiple-band alignments in a high-temperature ferromagnetic Mg(OH)<sub>2</sub>/VS<sub>2</sub> heterobilayer. *Phys Rev B*, 2017, 95, 245408
- [48] Du J, Xia C, Xiong W, et al. Two-dimensional transition-metal dichalcogenides-based ferromagnetic van der Waals heterostructures. *Nanoscale*, 2017, 9, 17585
- [49] Zhang Z, Ni X, Huang H, et al. Valley splitting in the van der Waals heterostructure WSe<sub>2</sub>/CrI<sub>3</sub>: The role of atom superposition. *Phys Rev B*, 2019, 99, 115441
- [50] Farooq M U, Hong J. Switchable valley splitting by external electric field effect in graphene/CrI<sub>3</sub> heterostructures. *npj 2D Mater Appl*, 2019, 3, 3
- [51] Zhang J, Zhao B, Zhou T, et al. Strong magnetization and Chern insulators in compressed graphene/CrI<sub>3</sub> van der Waals heterostructures. *Phys Rev B*, 2018, 97, 085401
- [52] Zhang H, Qin W, Chen M, et al. Converting a two-dimensional ferromagnetic insulator into a high-temperature quantum anomalous Hall system by means of an appropriate surface modification. *Phys Rev B*, 2019, 99, 165410
- [53] Gong C, Zhang X. Two-dimensional magnetic crystals and emergent heterostructure devices. *Science*, 2019, 363, 706
- [54] Mak K F, McGill K L, Park J, et al. The valley Hall effect in MoS<sub>2</sub> transistors. *Science*, 2014, 344, 1489
- [55] Seyler K L, Zhong D, Huang B, et al. Valley manipulation by optically tuning the magnetic proximity effect in WSe<sub>2</sub>/CrI<sub>3</sub> heterostructures. *Nano Lett*, 2018, 18, 3823
- [56] Aivazian G, Gong Z, Jones A M, et al. Magnetic control of valley pseudospin in monolayer WSe<sub>2</sub>. *Nat Phys*, 2015, 11, 148
- [57] Peng R, Ma Y, Zhang S, et al. Valley polarization in janus single-layer MoSSe via magnetic doping. *J Phys Chem Lett*, 2018, 9, 3612
- [58] Pei Q, Zhou B, Mi W, et al. Triferroic material and electrical control of valley degree of freedom. *ACS Appl Mater Interfaces*, 2019, 11, 12675
- [59] Sun W, Wang W, Chen D, et al. Valence mediated tunable magnetism and electronic properties by ferroelectric polarization switching in 2D FeI<sub>2</sub>/In<sub>2</sub>Se<sub>3</sub> van der Waals heterostructures. *Nanoscale*, 2019, 11, 9931